Chapter 4

Dissimilar Material-based Multistage Thermoelectric Generator with Varying Leg Geometry

Overview: This chapter presents a modified thermoelectric generator (TEG) featuring a two-stage configuration with variable leg geometry and dissimilar thermoelectric materials. A comprehensive iterative model is developed to analyze its performance under varying operating conditions. The study examines the influence of row number, exhaust inlet temperature, and coolant flow on key performance parameters, including voltage, power output, conversion efficiency, and their normalized counterparts. To optimize thermal performance, a varying cross-section is employed on the cold side to induce a more pronounced temperature gradient compared to a uniform geometry. The objective is to identify the optimal configuration that maximizes the efficiency and output of the multistage variable-shape thermoelectric generator (MVS-TEG).

4.1 Mathematical Modeling of MVS-TEG

Fig. 4.1 shows the newly designed multistage-variable shape TEG (MVS-TEG) designed for the present study. The first stage is comprised of the constant cross-section while the preceding stage is a variable one. A varying cross-section is employed because it ensures a greater temperature gradient as compared to a constant cross-section on the cold side. Fig. 4.2 shows the schematic of the complete system comprising the parallel heat exchangers, the computational units, and the direction system used. The grey strips in between the flat and converging legs in figure 4.1 has been used to differentiate the different stages. Table 4.1 lists the thermoelectric properties of the MVS-TEG **(**Massetti

et al., 2021). Parallel flow is preferred per the findings of Bejan et al. (2014). The system consists of a heat exchanger at the hot side, then the MVS TEG, and eventually the coolant channel at the cold side of the generator. When exhaust gas flows through the exhaust heat exchanger, the TEG experiences heat input at the hot side and cold at the cold side due to coolant. A potential difference due to temperature difference is produced. With time, the temperatures at the terminals achieve a steady state, and a steady flow of current is also reached.

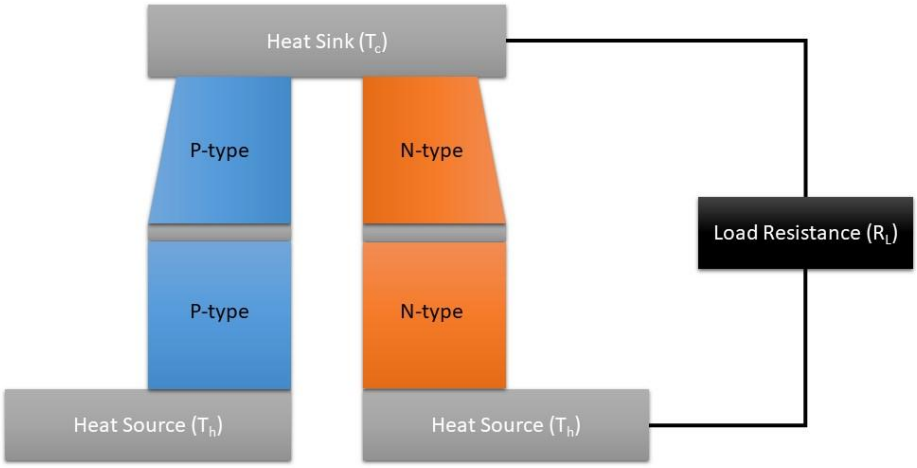

Fig. 4.1 Schematic Diagram of MVS-TEG

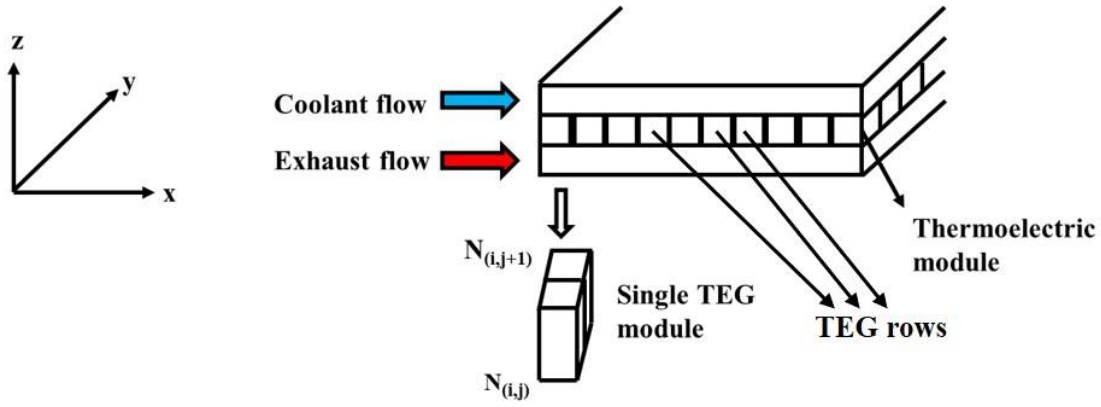

Fig. 4.2 Schematic Diagram of fluid flow and TEG system

The MVS-TEG is modeled on various energy conservation assumptions. Firstly, heat transfer attains a steady state across the TEG, which implies that the heat gained by the hot side of the TEG from the exhaust and the heat lost by the cold side of the TEG to the coolant is the same, respectively. Radiative heat transfer of any kind and heat transfer in the ducts are also neglected. The contact resistances between fluids and heat source and sink are neglected. The Thomson effect is disregarded because of the constant transport properties (α, ρ, k). The boundary conditions for the TEG are $x = 0 \rightarrow T = T_h$ and $x = h \rightarrow T = T_c$.

Table 4.1: Thermoelectric characteristics of p-type and n-type TEG materials (Massetti et al., 2021b)

TEG Material	Thermal conductivity (W/m K)	Seebeck coefficient (μV/K)	Electrical Conductivity (S/cm)	Figure of Merit (ZT)
P-type				
PEDOT/Bi_2Te_3	0.7	165	500	0.58
PEDOT:PSS	0.33	73	880	0.42
N-type				
Poly [Kx(Ni-ett)] (1)	0.31	-151.7	64	0.2
Poly [Kx(Ni-ett)] (2)	0.84	-150	310	0.32

Based on the above assumptions, the governing equations for the heat transfer across the MVS-TEG are as follows (Sun et al., 2014):

$$Q_{i,h} = N_y \left[\alpha_{pn} I T_{i,h} + k_{pn}\left(T_{i,h} - T_{i,m}\right) - \frac{I^2 R_{pn}}{2} \right] \tag{4.1}$$

$$Q_{i,m} = N_y \left[\alpha_{pn} I T_{i,m} + k_{pn}\left(T_{i,h} - T_{i,m}\right) + \frac{I^2 R_{pn}}{2} \right] \tag{4.2}$$

$$Q_{i,m} = N_y \left[\alpha_{pn} I T_{i,m} + k_{pn}\left(T_{i,m} - T_{i,c}\right) - \frac{I^2 R_{pn}(z)}{2} \right] \tag{4.3}$$

$$Q_{i,c} = N_y \left[\alpha_{pn} I T_{i,c} + k_{pn}\left(T_{i,m} - T_{i,c}\right) - \frac{I^2 R_{pn}(z)}{2} \right] \tag{4.4}$$

Where N_y, I, and T represent the number of legs along the y-direction, steady-state current, and temperatures respectively. The above equations consider the Peltier effect, the Joule effect, and thermal conduction losses. The different thermoelectrical properties are as follows (Sahoo and Karana, 2020):

$$\alpha_{pn} = \alpha_p - \alpha_n \tag{4.5}$$

$$k_{pn} = \frac{lb(\beta_p - \beta_n)}{h} \tag{4.6}$$

$$R_{pn} = \frac{h(\rho_p - \rho_n)}{lb} \tag{4.7}$$

Where α, k, R, l, b, h, and ρ denotes the Seebeck coefficient, thermal conductivity, electrical resistance, length, breadth, and height of the TEG leg, and resistivity of the TEG material respectively. The thermoelectric module is composed of several TEGs which are connected in series electrically and parallel thermally. For analysis purposes, the module is divided into N_x and N_y calculation units along the x-axis and y-axis respectively. Considering the variable cross-section of the second stage, we have:

$$A(z) = A_0 \left(\frac{h - {}^{z}/_{2}}{h} \right) \tag{4.8}$$

Where areas $A_0 = lb$ and $A(z) = l(z)b$. Thus, we have:

$$l(z) = l\left(\frac{h - {}^{z}/_{2}}{h}\right) \tag{4.9}$$

Based on the above geometry of the latter stage, the thermoelectric property varies as follows:

$$k_{pn}(z) = \frac{l(z)b(\beta_p - \beta_n)}{h} \tag{4.10}$$

$$R_{pn}(z) = \frac{h(\rho_p - \rho_n)}{l(z)b} \tag{4.11}$$

Table 4.2 enlists the fluid flow and thermophysical properties of the exhaust gas and coolant **(**Karana and Sahoo, 2018**)**. The heat exchange between the different fluids follows Newton's law of cooling:

$$Q_{i,h} = N_y h_{ex} A_{TEG,h}\left(T_{ex,avg} - T_{i,h}\right) \tag{4.12}$$

$$Q_{i,c} = N_y h_{co} A_{TEG,c}\left(T_{i,c} - T_{co,avg}\right) \tag{4.13}$$

Table 4.2: Thermal and flow properties of exhaust gas and coolant

Property	Value
Mass flow rate of exhaust gas	0.03kg/s
Specific heat of exhaust gas	1020J/kgK
Exhaust gas heat transfer coefficient	80W/m^2 K
Specific Heat of coolant	4180J/kgK

Also, assuming smooth walls of the coolant channel, the suitable Nusselt number and friction factor correlation used for the study are as follows (Bergman et al., 2011):

$$Nu = \frac{(f/8)(Re - 1000)Pr}{1 + 12.7(f/8)^{1/2}(Pr^{2/3} - 1)} \tag{4.14}$$

$$f = (0.79 \ln Re - 1.64)^{-2} \tag{4.15}$$

When the system attains a steady state, the heat lost by exhaust gas equals the heat gained on the hot side, and the heat lost by the cold side equals the heat gained by the coolant.

$$Q_{i,h} = \dot{m}_{ex} c_{p,ex} (T_{i+1,ex} - T_{i,ex}) \tag{4.16}$$

$$Q_{i,c} = \dot{m}_{co} c_{p,co} (T_{i,co} - T_{i+1,co}) \tag{4.17}$$

As the exhaust gas and coolant flow across the module, the temperature gradient causes the production of potential across the two sides of the TEG. The potential developed is a function of the thermoelectric property and the temperature difference between the hot and cold sides, also known as the Seebeck effect:

$$V_i = N_y \alpha_{pn} \left(T_{i,h} - T_{i,c}\right) \tag{4.18}$$

Hence, the total output voltage is given as:

$$V_{Total} = N_y \alpha_{pn} \sum_{1}^{N_x} \left(T_{i,h} - T_{i,c}\right) \tag{4.19}$$

The combined resistance offered by the TEG and resistance load gives the current I_c with the help of Ohm's law.

$$R_{eq} = N_x N_y R_{pn} + R_L \tag{4.20}$$

$$I_c = V_{Total} / R_{eq} \tag{4.21}$$

Another critical parameter, demonstrating the utility of the TEG is the power produced, which can be calculated as follows:

$$P = I_c^2 R_L \tag{4.22}$$

To understand the benefit of the TEG, the output relative to the heat input is measured, which is commonly known as conversion efficiency:

$$\eta_{conv} = \frac{P}{\sum_i^{N_x}(Q_{i,h})} \tag{4.23}$$

Now, the maximum current occurs when the load resistance, $R_L = 0$ (Sahoo and Karana, 2020). Thus, the expression for maximum parameters like output voltage and power are:

$$V_{max} = \alpha_{pn}(T_h - T_c) \tag{4.24}$$

$$Power_{max} = \alpha_{pn}^2(T_h - T_c)^2/4R_{TEG} \tag{4.25}$$

However, the maximum efficiency of the TEG is given by:

$$\eta_{max} = \frac{\left(1 - {}^{T_c}/_{T_h}\right)\sqrt{1+ZT} - 1}{\sqrt{1+ZT} - {}^{T_c}/_{T_h}} \tag{4.26}$$

The second law efficiency of the device is also ascertained to quantify its exergetic performance with the help of the following equations:

$$\eta_{II} = \frac{Power}{Power + I_{rr}} \tag{4.27}$$

$$I_{rr} = T_0 S_{gen} \tag{4.28}$$

$$S_{gen} = \frac{Q_h}{T_h} - \frac{Q_c}{T_c} \tag{4.29}$$

Where I_{rr} is the irreversibility associated with the heat transfer across the TEG while S_{gen} is the entropy generated at the same condition of flow. For the present theoretical research, the following nomenclature has been employed as shown in Table 4.3. An iterative approach is developed for steady-state calculations with the help of Energy Equation Solver (EES) software. The algorithm utilized is shown in Fig. 4.3. The material poly[Kx(Ni-ett)](1) is poly(Nickel 1,1,2,2-ethylenetetrathiolate) while poly[Kx(Ni-ett)](2) is electrochemically treated poly(Nickel 1,1,2,2-ethylenetetrathiolate).

Table 4.3: Nomenclature of the generators under study

Combination no.	P-type material	N-type material
MVS TEG 1	PEDOT/Bi_2Te_3	poly[Kx(Ni-ett)] (1)
MVS TEG 2	PEDOT/Bi_2Te_3	poly[Kx(Ni-ett)] (2)
MVS TEG 3	PEDOT:PSS	poly[Kx(Ni-ett)] (1)
MVS TEG 4	PEDOT:PSS	poly[Kx(Ni-ett)] (2)

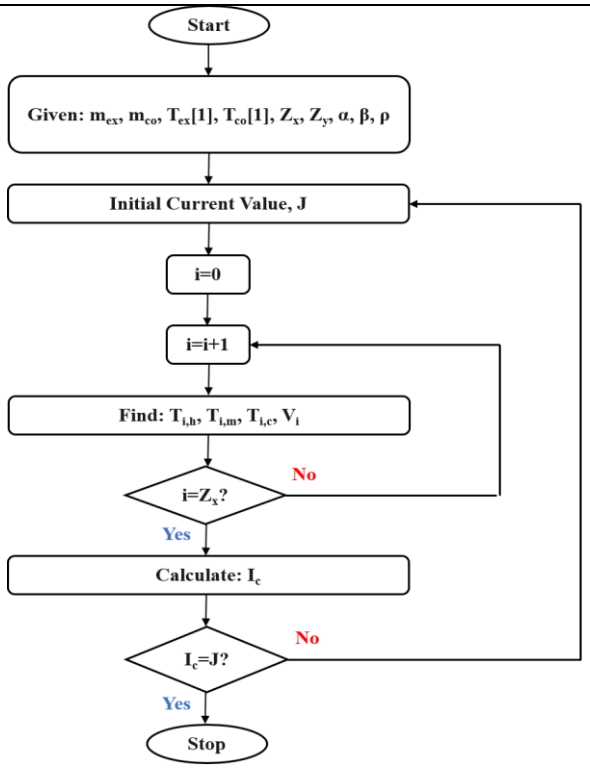

Fig. 4.3 Iterative approach employed in the current study

The validation of the proposed new configuration has been done with the published data (Karana and Sahoo, 2019), and shown in Fig. 4.4. The exhaust and coolant temperatures are found to be following a similar trend with some deviation that occurs due to different initial conditions. The average error in prediction of ΔT across the TEG is 1.54%.

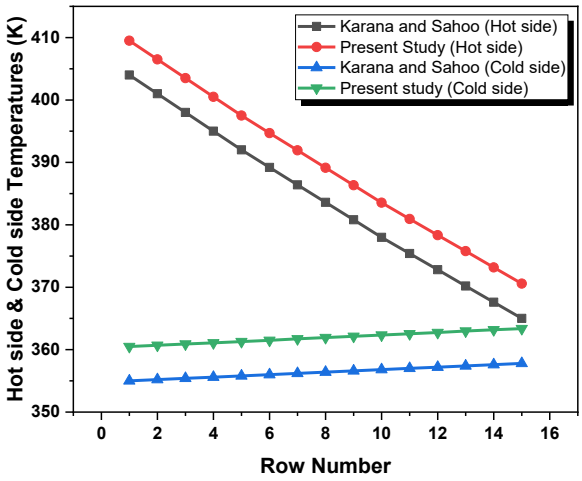

Fig. 4.4 Validation of the present study with the published study

4.2 Results and Discussion

4.2.1 Variation in TEG performance with number of rows

Variation of voltage produced for an exhaust flow rate of 0.03kg/s and exhaust inlet temperature condition of 500K with the row number for different MVS-TEG combinations is shown in Fig. 4.5. From the result obtained, it can be observed that voltage increases as the row number increases. However, the rate of increase in the voltage produced keeps on decreasing in the direction of the flow. It is because as the exhaust and coolant advance their flow across the MVS-TEG system, the temperature difference between the hot side and cold side of the MVS-TEG decreases. This fall in the temperature difference between the two sides of the MVS-TEG is because as both fluids flow, the exhaust loses its heat content while the coolant is heated along the flow. This decreases the exhaust temperature while the coolant temperature rises. Now, the main cause behind the development of the voltage is the existence of the temperature gradient. As this gradient decreases along the flow, this results in lower voltage production of the TEG module.

From the outcome, it can also be deduced that the highest voltage is produced by MVS TEG-2 followed by MVS TEG-1, MVS TEG-4, and MVS TEG-3. The voltage increases by 8.405, 8.505, 8.316, and 8.373 times for MVS TEG-1, MVS TEG-2, MVS TEG-3, and MVS TEG-4 respectively of the voltage produced by the generators in the first row. Also, a critical point to be noted is that an optimum value of the TEG is observed as 19 for MVS TEG-1, MVS TEG-3, and MVS TEG-4, and 18 for MVS TEG-2. This helps us in defining the maximum number of useful rows for the application.

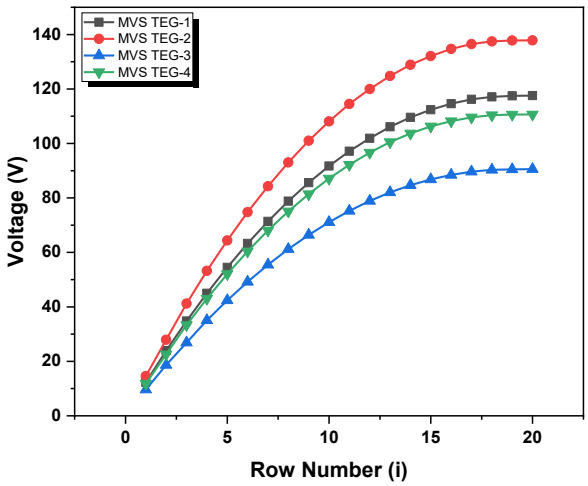

Fig. 4.5 Voltage v/s Row number

Fig. 4.6 shows the effect of row number on the power developed by the different MVS-TEG systems for 0.03kg/s exhaust flow rate and 500K exhaust inlet temperature. The power developed increases rapidly with the row number. However, this increment is soon retarded and a lower power generation rate is seen by further increasing the generator's row. This decrement is such that after a particular row, the MVS-TEG produces lesser power in comparison with the row just before it.

This is because power generation is highly dependent on the temperatures of the exhaust and coolant on the hot and cold side of the MVS-TEG respectively. The temperature gradient causes the motion of electrons and holes throughout the TEG system

resulting in the Seebeck effect, Joule's effect, and thermal conduction of heat. The result is the generation of a certain amount of power across the resistance load. However, on adding a greater number of rows beyond a certain limit, the power generation falls. This gives the optimum row number that must be utilized and helps to determine the nominal size of the module. Also, it is observed that the maximum power is generated by MVS TEG-2, followed by MVS TEG-1, MVS TEG-4, and MVS TEG-3. The increment is 8.406, 8.508, 8.313, and 8.37 folds for MVS TEG-1, MVS TEG-2, MVS TEG-3, and MVS TEG-4 respectively.

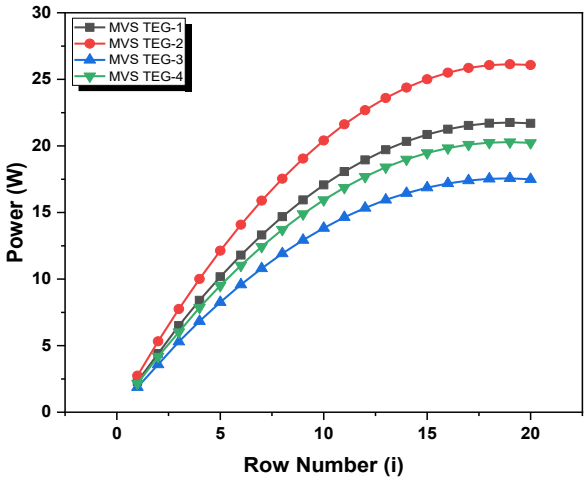

Fig. 4.6 Power v/s Row number

The variation of conversion of different MVS-TEG for the exhaust flow rate and inlet temperature for the coolant flow rate of 0.03kg/s and inlet temperature of 298K is shown in Fig. 4.7. The conversion efficiency of all the MVS-TEG is observed to decrease with the row number. This may be due to lower power generation relative to the heat supplied to the hot side of the MVS-TEG. As the row number is increased, it is seen that the exhaust temperature decreases which results in lower heat supplied. However, simultaneously, the power generation decreases due to lower temperatures along the flow direction. Also, different thermoelectrical properties result in varying performances of the

generators. MVSTEG-2 was able to convert maximum heat into power among the different MVS-TEGs considered in the theoretical study. The conversion efficiency is found to be lower for the subsequent generators in MVS TEG-1, MVS TEG-4, and MVS TEG-3 order. However, the parameter is found to fall by 50.32%, 49.86%, 50.76%, and 50.47% for MVS TEG-1, MVS TEG-2, MVS TEG-3, and MVS TEG-4. Thus, it can be remarked that the conversion efficiency falls by almost half for all the MVS-TEG. Also, MVS TEG-2 (p-type: PEDOT:Bi_2Te_3, n-type: poly[Kx(Ni-ett)](2)) not only exhibits the maximum conversion efficiency but also it displays the least decrement in it.

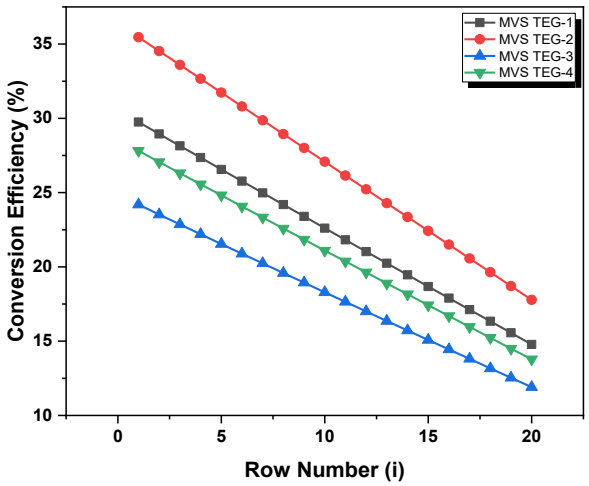

Fig. 4.7 Conversion efficiency v/s Row number

The second law efficiency of any device gives its exergetic performance concerning the different input variables. Fig. 4.8 shows the variation of the second law efficiency of different MVS-TEG with TEG unit row numbers for an exhaust flow rate of 0.03kg/s and 500K exhaust inlet temperature. The second law efficiency which is a measure of the irreversibility of the generator falls in a slightly non-linear fashion. This shows that the irreversibility increases along the exhaust flow direction. This is because as the row number is increased the rate of entropy generation increases because of more heat transfer across the system. The second law of efficiency incorporates the power

produced, heat transfers at both sides of the MVS-TEG, and their respective junction temperature. The second law efficiency decreases as the irreversibility increases due to a lower temperature gradient as the exhaust loses its heat content while the coolant gains heat from the generator.

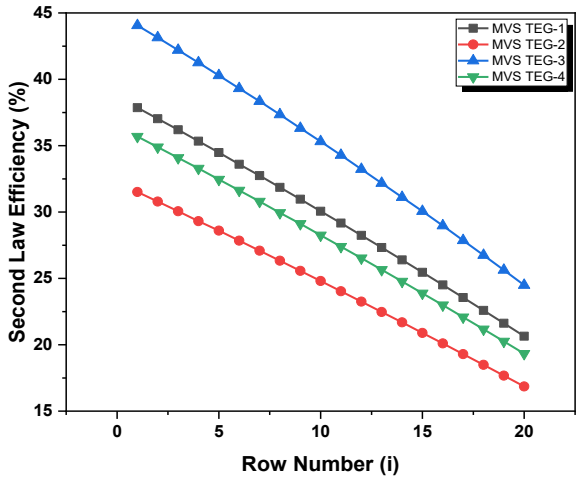

Fig. 4.8 Second law efficiency v/s Row number

Quantitatively, the second law efficiency decreases by 45.72%, 46.78%, 44.76%, and 46.1% for MVS TEG-1, MVS TEG-2, MVS TEG-3, and MVS TEG-4 respectively. MVS TEG-3 exhibits the maximum parameter value throughout while MVS TEG-2 shows the least. MVS TEG-1 and MVS TEG-2 display intermediate performance. However, it is observed that MVS TEG-3 exhibited the best performance parameter over other generators concerning the input variables and hence, this TEG is appreciated over others.

Besides output performance parameters (voltage, power, and conversion efficiency), it is important to ascertain how the generator performed relative to its maximum performance. It helps to find out how much the device has scope to improve. For this, normalized parameters become very crucial to calculate. Fig. 4.9 shows the normalized voltage variation with the row number for 0.03kg/s exhaust flow rate and

500K exhaust inlet temperature. The parameter decreases gradually till the second-row number for all generators after which it falls linearly. This decrement implies that all the MVS-TEGs have a greater potential for voltage generation at higher row numbers since the later TEG rows operate under lower hot side temperatures and higher coolant temperatures. It happens because of the decrement in temperature gradient across every row. At higher row numbers, a lower temperature gradient results in the above-mentioned decrement.

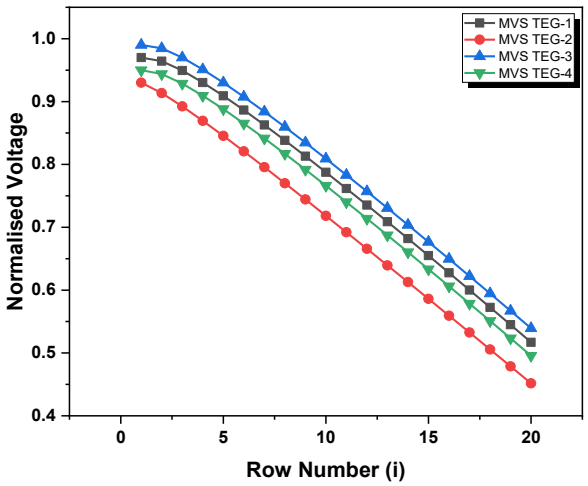

Fig. 4.9 Normalized voltage v/s Row number

The results exhibit that MVS TEG-3 (p-type: PEDOT/PSS, n-type: poly[Kx(Ni-ett)] (1)) displays the best overall performance in voltage generation as it has the highest parameter value. Furthermore, the normalized voltage decreases by 46.7%, 51.4%, 45,5%, and 47.8% for MVS TEG 1, 2, 3, and 4 respectively.

The effect of row number on the normalized power is shown in Fig. 4.10. Normalized power slopes downward slowly until the second row after which it reduces close to half of its initial value for all the MVS-TEG. Even though the power developed was observed to increase as shown in Fig. 4, when compared to the maximum power

output, it decreases. This implies that in comparison to maximum power, actual power produced decreases with row number.

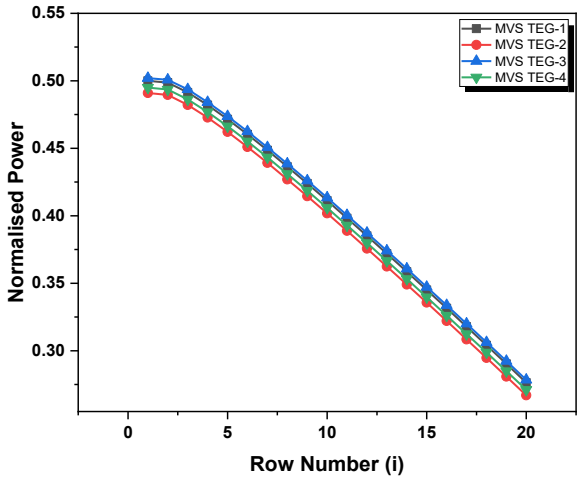

Fig. 4.10 Normalized Power v/s Row number

This trend is also observed to follow the results of the power versus row number where the power output is in the following order: MVS TEG-3, MVS TEG-1, MVS TEG-4, and MVS TEG-2. The normalized power decreases by 44.72%, 45.61%, 44.52, and 45.23% for MVS TEG-1, MVS TEG-2, MVS TEG-3, and MVS TEG-4 respectively. Normalized power values of the generators lie very close meaning that with the variation in row number under the same boundary and initial conditions, the generator gives similar normalized performance quantitatively.

On drawing a comparison of the normalized conversion efficiency of the different MVS-TEGs against row number, it is observed that the parameter decreases, signifying that the generators could have converted the heat more efficiently along the flow. This effect is made known in Fig. 4.11. The maximum conversion efficiency is the function of the Figure of merit (Z) and means temperature or dimensionless Figure of merit (ZT) in general. However, conversion efficiency depends on the actual performance of the generators governed exclusively by temperature. Thus, as the difference between the hot

side and cold side of the MVS-TEG decreases, conversion efficiency decreases. A point worth noting here is the decrement in the normalized conversion efficiency. The reason is that the decrement in conversion efficiency is more pronounced than its maximum counterpart. The constraint value decreases by 51.98%, 49.86%, 49.94%, and 55.42% for MVS TEG-1, MVS TEG-2, MVS TEG-3, and MVS TEG-4 respectively.

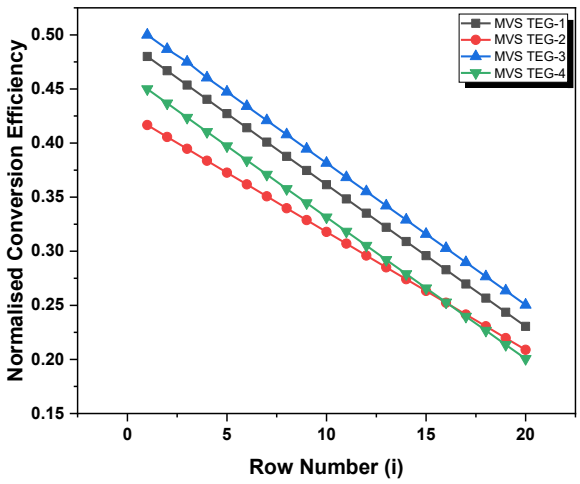

Fig. 4.11 Normalized conversion efficiency v/s Row number

Thus, the best action is exhibited by MVS TEG-3, followed by MVS TEG-1, MVS TEG-4, and MVS TEG-2. However, MVS TEG-2 (p-type: PEDOT/Bi_2Te_3, n-type: poly[Kx(Ni-ett)] (2)) performs better than MVS TEG-4(p-type: PEDOT:PSS, n-type: poly[Kx(Ni-ett)] (2)) for row number 17 and above.

4.2.2 Variation in TEG performance with exhaust inlet temperature

Fig. 4.12 shows the variation of voltage concerning the exhaust inlet temperature. The exhaust inlet temperature plays an important role in the MVS-TEG performance as it alters the end temperatures of the generators and hence the output. With the increase in exhaust temperature, the voltage produced by the MVS-TEG increases. It happens because the overall heat transfer rate increases which helps in creating higher temperature gradients along the flow. Maximum voltage is produced by MVS TEG-2, followed by

MVS TEG-1, MVS TEG-4, and MVS TEG-3. The voltage developed rises by 54%, 56.5%, 57.4%, and 58.9% for MVS TEG-1, MVS TEG-2, MVS TEG-3, and MVS TEG-4 respectively when the exhaust inlet temperature variation is studied from 450K to 545K. Overall, exhaust temperature increment raises the voltage performance. However, MVS TEG-2 has the maximum voltage because of the highest thermoelectric properties of p-type PEDOT/Bi_2Te_3 and n-type poly[Kx(Ni-ett)] (2).

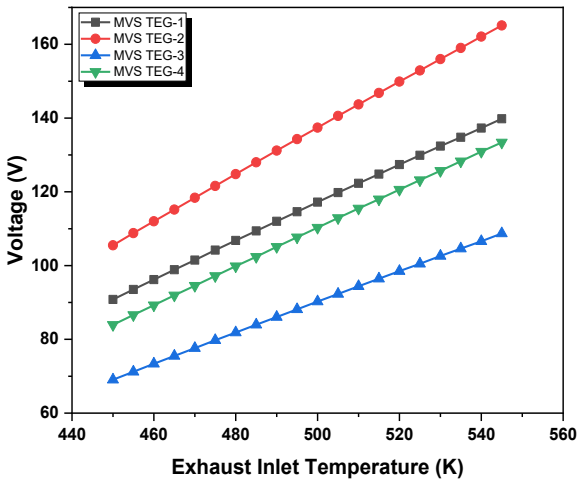

Fig. 4.12 Voltage v/s Exhaust inlet temperature

The power developed by the generators increases as the exhaust temperature is increased (Fig. 4.13). With higher temperature as the initial condition, the generators capture to work in a higher temperature zone. This enhances the Seebeck effect which is responsible for voltage and power generation. Not only does Seebeck power increase but also the heat conducted across the MVS-TEG rises which results in more heat loss due to the negative impact of electron and hole movement. However, fortunately, the Seebeck effect overwhelms the other performance-hampering traits of the material due to improved thermoelectric properties and Figures of merit. The tapering and multi-staging effect further enhance this action. Talking of the quantitative performance, MVS TEG-2 (p-type: PEDOT:Bi_2Te_3, n-type: poly[Kx(Ni-ett)] (2)) produces maximum power while

MVS TEG-3 (p-type: PEDOT/PSS, n-type: poly[Kx(Ni-ett)] (1)) produces the least. The increments in power development with the exhaust temperature at the inlet for 0.03kg/s exhaust mass flow rate are 53%, 55.5%, 56.3%, and 57.9% for MVS TEG-1, MVS TEG-2, MVS TEG-3, and MVS TEG-4 respectively.

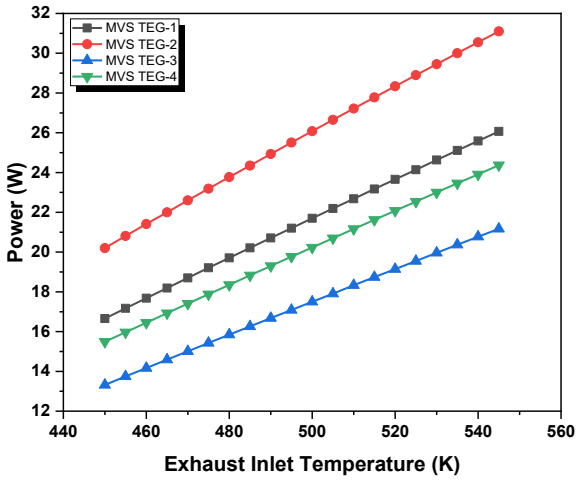

Fig. 4.13 Power v/s Exhaust inlet temperature

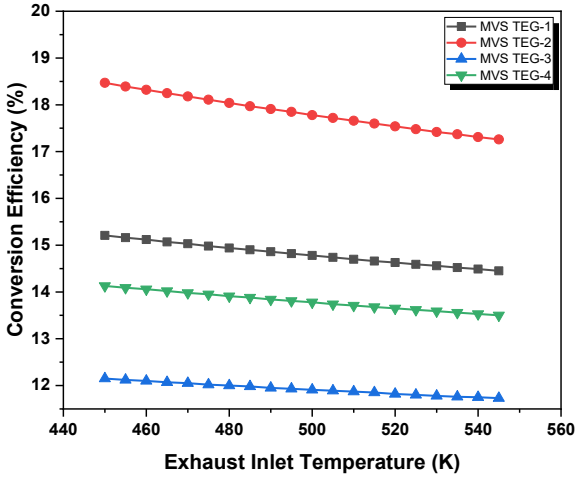

Fig. 4.14 Conversion efficiency v/s Exhaust inlet temperature

Fig. 4.14 shows the effect of exhaust inlet temperature on the conversion efficiency for 0.03Kg/s exhaust and coolant flow rate for exhaust temperature variation from 450K to 545K. With the temperature increase, the conversion efficiency decreases

because the increment in power generation is overpowered by enhanced heat transfer. The thermoelectric conversion efficiency decreases by 5%, 6.55% 3.46%, and 4.46% for MVS TEG-1, MVS TEG-2, MVS TEG-3, and MVS TEG-4 respectively. Thus, the employment of multiple-stage and variable cross-sections with novel materials not only helps to lower the efficiency losses but also helps achieve high values that have not been seen in conventional TEG with single-leg material of bismuth telluride. Therefore, the use of dissimilar materials with suitable characteristics is encouraged in the present study.

The effect of exhaust inlet temperature on the second law efficiency for different MVS-TEG at an exhaust flow rate of 0.03kg/s is negligible as the heat transfer rates vary per the temperatures at the generator ends. This is exhibited in Fig. 4.15. Maximum decrement is exhibited by MVS TEG-3 even though it inherits the highest second-law efficiency throughout the temperature range. However, the second law efficiency falls by 3.34%, 1.98%, 4.75%, and 2.87% for MVS TEG-1, MVS TEG-2, MVS TEG-3, and MVS TEG-4 respectively.

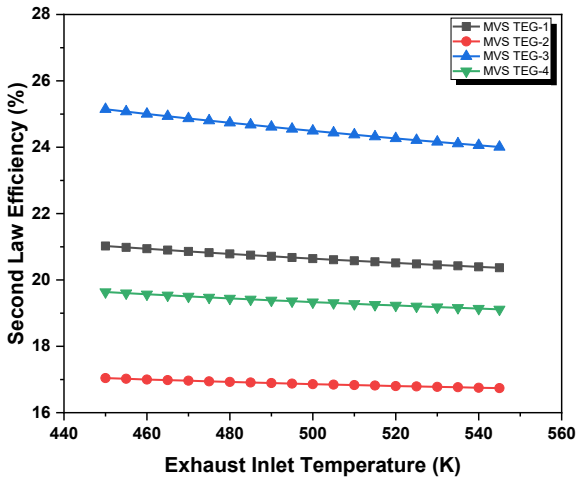

Fig. 4.15 Second law efficiency v/s Exhaust inlet temperature

However, the significant gap between individual second law efficiencies occurs due to distinct Seebeck coefficient, electrical conductivity, and thermal conductivity.

Overall, the effect of exhaust temperature is more noticeable over voltage and power while other factors are trivially affected. The decrease in normalized voltage with exhaust temperature for the previously mentioned inlet and initial conditions is displayed in Fig. 4.16. Contrary to other outputs subjected to similar conditions, the normalized voltage is very least affected by the change in exhaust inlet temperature. This means that the voltage developed and the maximum voltage run together throughout the temperature variation. It happens because as exhaust inlet temperature is increased, the maximum voltage that can be produced overpowers the actual voltage produced. The generators exhibit maximum normalized voltage at the minimum exhaust temperature. The parameter value decreases by 0.2%, 0.3%, 0.2%, and 0.2% respectively for MVS TEG-1, MVS TEG-2, MVS TEG-3, and MVS TEG-4.

The variation of the normalized power for different exhaust inlet temperatures is shown in Fig. 4.17 for different MVS-TEGs. It is observed that the normalized power decreases with the increase in exhaust inlet temperature. The reason is the falling rate of power generation relative to maximum power because of improved hot side temperature. The parameter value decreases by 0.19%, 0.26%, 0.15%, and 0.19% for MVS TEG-1, MVS TEG-2, MVS TEG-3, and MVS TEG-4 respectively under the exhaust flow rate of 0.03kg/s. However, MVS TEG-3 exhibits better performance than MVS TEG-1 for exhaust inlet temperatures of 530K and above. Also, MVS TEG-4 (p-type: PEDOT:PSS, n-type: poly[Kx(Ni-ett)] (2)) performs second to MVS TEG-2 (p-type: PEDOT/Bi_2Te_3, n-type: poly[Kx(Ni-ett)] (2)) up to 545K, though it appears that it may provide better results than MVS TEG-2 above this temperature.

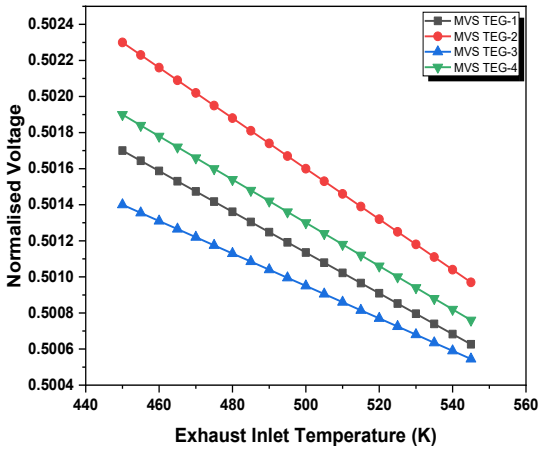

Fig. 4.16 Normalized voltage v/s Exhaust inlet temperature

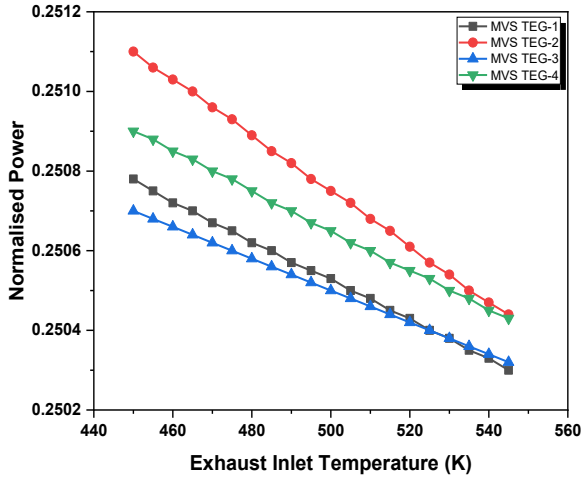

Fig. 4.17 Normalized Power v/s Exhaust inlet temperature

The effect of exhaust inlet temperature on the normalized parameter of conversion efficiency is depicted in Fig. 4.18 for the exhaust flow rate of 0.03kg/s. The normalized conversion efficiency falls as the exhaust inlet temperature rises. There is a negligible fall in the Parameter value which shows its weak reliance on the input variable under study. The normalized conversion efficiency decreases by 0.2%, 0.27%, 0.16%, and 0.2% for MVS TEG-1, MVS TEG-2, MVS TEG-3, and MVS TEG-4 respectively.

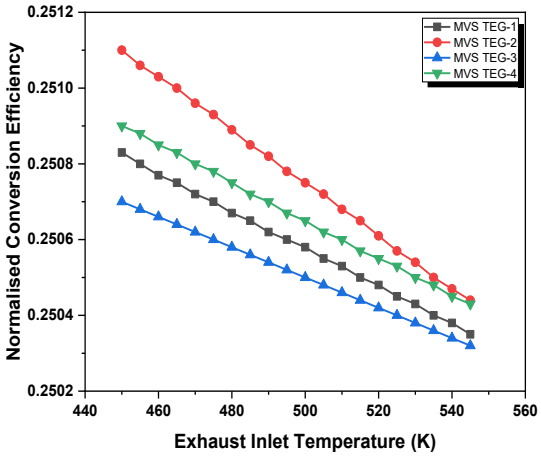

Fig. 4.18 Normalized conversion efficiency v/s Exhaust inlet temperature

However, a close observation would tell us that the MVS TEG-2 and MVS TEG-4 perform better for all the normalized parameters when the exhaust inlet temperature is varied. Also, the normalized parameters appear to be negligibly influenced by the variation in exhaust temperature.

4.2.3 Variation in TEG performance with the coolant flow rate

The variation of voltage produced with the coolant flow rate is shown in Fig. 4.19. With the increase in coolant flow rate, the heat transfer rate at the cold side of the MVS-TEG increases. This, coupled with muti-staging and tapering cross-section of the second stage enhances the cooling rate, which eventually results in increased voltage production. Faster coolant flow carries away more heat and thus higher temperature gradient results in more voltage production. MVS TEG-2 produces the highest voltage. MVS TEG-1, MVS TEG-4, and MVS TEG-3 come subsequent in action after MVS TEG-1. However, the increment in output is by 7.8%, 7.4%, 7.2%, and 6.9% in MVS TEG-1, MVS TEG-2, MVS TEG-3, and MVS TEG-4 respectively.

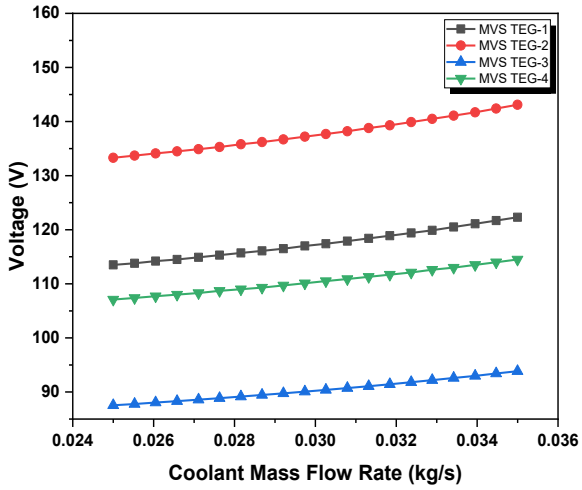

Fig. 4.19 Voltage v/s Coolant flow rate

When the coolant flow rate is raised, the increase in cold side temperature along the flow across the MVS-TEG is reduced which marks the occurrence of higher power production. This trend is observed in Fig. 4.20. Overall maximum power is generated by MVS TEG-2 which increases by 7.8%. MVS TEG-1, MVS TEG-4, and MVS TEG-3 are next in line with 7.4%, 7.2%, and 6.9% increments in power generation. Maximum power is produced by MVS TEG-2(p-type: PEDOT:Bi_2Te_3, n-type: poly[Kx(Ni-ett)] (2)).

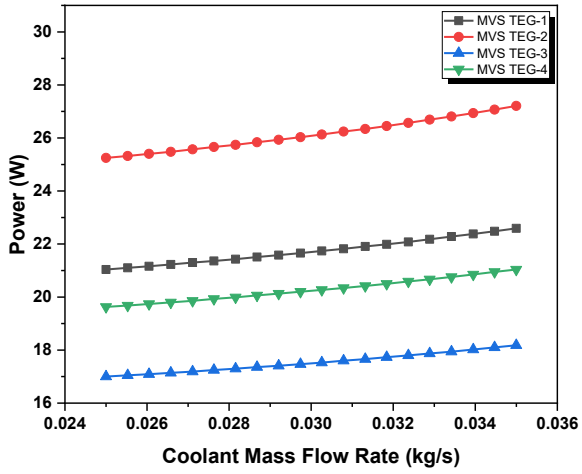

Fig. 4.20 Power v/s Coolant flow rate

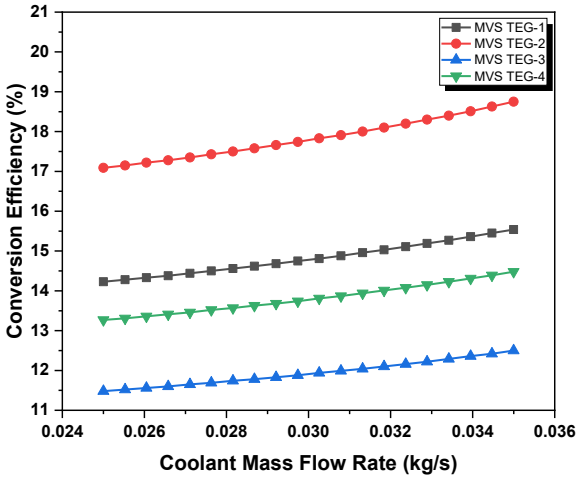

Fig. 4.21 Conversion efficiency v/s Coolant flow rate

Fig. 4.21 shows the effect of coolant flow rate on the conversion efficiencies of different MVS-TEG for 0.03kg/s and 500K exhaust flow rate and inlet temperature. Conversion efficiency increases as the coolant flow rate is varied. This happens because a higher cooling rate due to increased flow rate cools the cold side of MVS-TEG better and greater conversion efficiency is obtained as a result of a higher temperature gradient. The best performance is exhibited by MVS TEG-2 (p-type: PEDOT:Bi_2Te_3 and n-type: poly[Kx(Ni-ett)] (2)) followed by MVS TEG-1, MVS TEG-4, and MVS TEG-3. The increment in conversion efficiencies is by 9.2%, 9.71%, 8.88%, and 9.12% respectively for MVS TEG-1, MVSTEG-2, MVSTEG-3, and MVSTEG-4.

The variation of second law efficiency when the coolant flow rate is changed from 0.025 to 0.035kg/s is for different MVS-TEG at an exhaust flow rate of 0.03kg/s, the exhaust inlet temperature of 500K, and coolant flow rate of 0.03kg/s is shown in Fig. 4.22. The second law efficiency decreases by 9.13%, 8.98%, 10.33%, and 9.04% for MVS TEG-1, MVS TEG-2, MVS TEG-3, and MVS TEG-4 respectively. This happens because an increased coolant flow rate increases the overall entropy generation due to heat

transfer. However, the most efficient irreversibility action is exhibited by MVS TEG-3 while MVS TEG-2 is the worst.

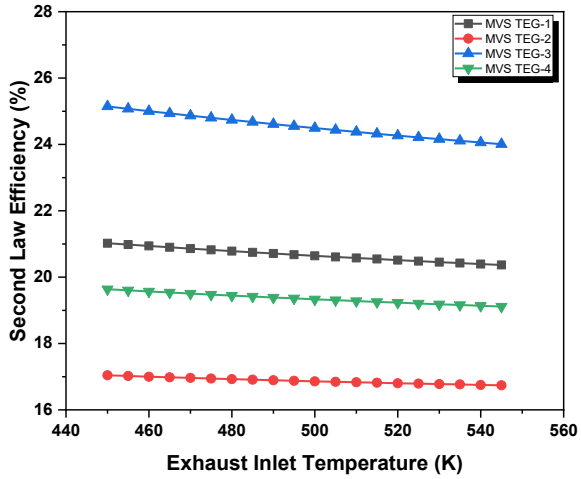

Fig. 4.22 Second law efficiency v/s Coolant flow rate

The variation of normalized parameters against coolant flow rate for different MVS-TEG considered under the theoretical study are shown in Fig. 4.23, and 4.24.

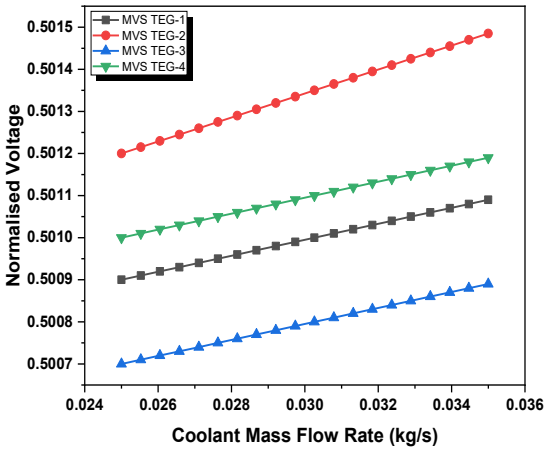

Fig. 4.23 Normalized voltage v/s Coolant flow rate

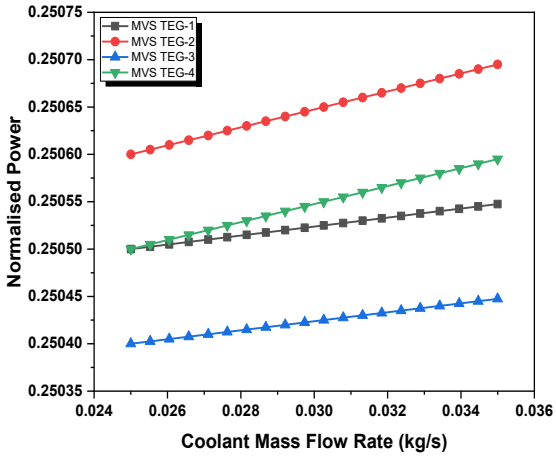

Fig. 4.24 Normalized power v/s Coolant flow rate

The normalized parameters display improved action with the coolant flow rate which is understandable due to the improved heat-carrying capacity of the coolant. The normalized voltage increases by 0.04%, 0.056%, 0.04%, and 0.038%; normalized power by 0.02%, 0.04%, 0.019%, and 0.041% for MVS TEG-1, MVS TEG-2, MVS TEG-3, and MVS TEG-4 respectively.

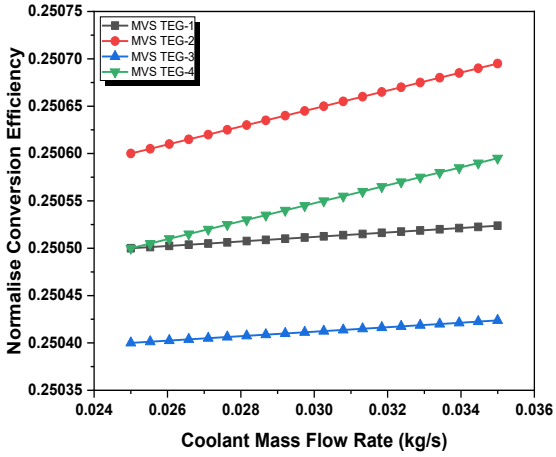

Fig. 4.25 Normalized conversion efficiency v/s Coolant flow rate

The effect of coolant flow rate on normalized conversion efficiency for different MVS-TEG at an exhaust flow rate and inlet temperature of 0.03kg/s and 500K, respectively, is shown in Fig. 4.25. The normalized conversion efficiency increases with

the coolant flow rate by 0.04% for both MVS TEG-2 and MVS TEG-4. However, it increases negligibly for MVS TEG-1 and MVS TEG-3.Thus, it is concluded that MVS TEG-3 performed the best for variation in generator row number, exhaust inlet temperature, and coolant flow rate. MVS TEG-1 occupies the second position followed by MVS TEG-4 and MVS TEG-2. Even though the transport characteristics of any material may seem healthier than the others, the effect of multi-staging and variable shape coupled with the dissimilar material combination is visible in the output parameters. The good output voltage, power, and most importantly conversion efficiency back the development of such a generator.

4.3 Highlights

- The results revealed that the most drastic effect is obtained when the row number is varied. Also, the work gives optimum values for voltage and power output as $N_x = 19$ for MVS TEG-1, MVS TEG-3, and MVS TEG-4 while $N_x = 18$ for MVS TEG-2.
- The novel MVS TEG also exhibited improved conversion efficiency, theoretically, over the conventional bismuth telluride generators. This justifies the implementation of multi-staging, tapering cross-section, and dissimilar material combinations with enhanced thermoelectric transport properties.
- The results show that exhaust inlet temperature conditions had a great influence on productivity parameters like voltage and power. The former varies by 54% to 59% and the latter by 53% to 58%.
- The second law efficiency falls by 3.12%, 1.77%, 4.53%, and 2.66% for MVS TEG-1, MVS TEG-2, MVS TEG-3, and MVS TEG-4 respectively.

- On average, the conversion efficiency increases by 9.23% for the different MVS TEG analyses in the theoretical work. However, it is observed that the second law efficiency decreases with the coolant flow rate.